Available online at www.sciencedirect.com

SciVerse ScienceDirect

Ceramics International 39 (2013) 8065–8072

CERAMICS INTERNATIONAL

www.elsevier.com/locate/ceramint

Production and structural characterization of tailored made open-cell alumina–vanadia foams

F. Stergioudi[a], G. Karelis[a], E. Paulidou[b], N. Michailidis[a,*]

[a]Physical Metallurgy Laboratory (PML), Mechanical Engineering Department, Aristotle University of Thessaloniki, 54124 Thessaloniki, Greece

[b]Solid State Section, Department of Physics, Aristotle University of Thessaloniki, 54006 Thessaloniki, Greece

Received 18 February 2013; received in revised form 24 March 2013; accepted 25 March 2013
Available online 6 April 2013

Abstract

Tailored made open-cell alumina–vanadia foams were produced by employing a dissolution sintering process, using crystalline raw cane sugar as a leachable pore former material. The process parameters of the production stages were properly adjusted to optimize the quality and structure of open-cell ceramic foams. The influence of sintering conditions (temperature, time and cooling rate) on the microstructure of the resultant foam is investigated with a view to produce high-quality ceramic foams having satisfactory strength. The effects of V_2O_5 molar addition on the microstructure of ceramics foams are described by SEM and XRD analyses. The crystal size, grain growth (appearance of texturing-preferred orientation) and X-ray intensities of phases are closely related to the cooling rate and sintering duration. V_2O_5 addition enlarges the lattice parameters of the Al_2O_3 phase resulting in a 4–5% increase of the actual (measured) porosity of the produced ceramic foam compared to the theoretical one.

Keywords: A. Sintering; B. X-ray methods; D. Al_2O_3; Ceramic foam

1. Introduction

The production of high porosity cellular materials has received increasing attention over the last decades mainly owing to interesting properties that they possess, such as high surface area, high permeability, low density and high thermal insulation [1,2]. So far alumina, mullite, zirconia and silicon carbide are the major material types from which ceramic foams have been manufactured in open- or closed-cell structures [1,3–7].

Open-cell ceramic foams are usually produced by ceramic replication of an organic substrate or by the space holder technique. In the replication method, which is the most widely used, an open-cell polymer template is infiltrated with a ceramic slurry and dried. Pyrolysis of the organics and sintering of the remaining ceramic body are the subsequent steps. The obtained product has a highly open structure but usually exhibits low mechanical strength due to the hollow struts and defects resulting from the polymer removal [1,3].

The space-holder technique consists of co-dispersing a ceramic powder with an easily burnable second phase, forming a green body, burning out the second phase and sintering the body. Cell size of the foam is easily controlled by the space-holder particle size distribution. As burning out of the space-holder leads to great amounts of gas; this process has to be controlled carefully [1,3].

Among porous ceramics, alumina foams have received a considerable amount of attention in recent years, because of the advantages that alumina offer in comparison with other ceramic materials: it is inexpensive, quite highly refractory with extremely high hardness and presents high chemical stability which confers resistance to corrosion, characteristics that make alumina foams eligible for use in a range of potential technological applications such as filtration processes, catalyst carriers and as porous implants in the field of biomaterials [3–6,8].

Nevertheless, most alumina foams suffer from poor stability and low strength attributed mainly to the high melting points, strong ionic bonds and low diffusion coefficient of alumina and therefore they require excessively prolonged heating cycles to acquire the desired strength of the final product. However, new methods are still being explored with a view to reduce the

*Corresponding author. Tel.: +30 2310 995891; fax: +30 2310 996069.
E-mail address: nmichail@eng.auth.gr (N. Michailidis).

0272-8842/$ - see front matter © 2013 Elsevier Ltd and Techna Group S.r.l. All rights reserved.
http://dx.doi.org/10.1016/j.ceramint.2013.03.078

sintering temperature and time so as to densify the final ceramic products. A significant number of studies have been dedicated on binders of alumina ceramics and modification of alumina powders in order to lower the sintering temperature, enhance compactibility of powders, and facilitate material shaping and machinability so as to improve the strength and quality of the produced ceramic product [3–6,9–11]. Addition of compounds promoting reaction sintering (due the creation of new phases) is also a well-known method to enhance properties of ceramic products and improve sinterability. Vanadium pentoxide (V_2O_5), widely used as a catalyst in industry for a variety of chemical reactions, is one of the most important metal oxides used to enhance both properties and sinterability (lower sintering temperature and duration) of the final ceramic product especially when catalysis is of importance [12–16]. For example, it has been reported that the addition of V_2O_5 reduces the temperature of the mullite phase formation in a mixture of Al_2O_3 and SiO_2 [12,15] whilst its mixture with TiO_2 or MoO_3 can act beneficially in improving the photo-catalytic activity and partial/selective oxidation catalysis, respectively [13,14,16].

In this study, a space-holder method for manufacturing open-cell alumina–vanadium oxide foams using crystalline raw cane sugar as a leachable pattern is reported. Crystalline raw cane sugar was successfully used as a pore former material for manufacturing Al-foams by a dissolution-sintering process [17,18]. However, to the best of our knowledge, sugar has not been reported in literature as a pore former material for manufacturing ceramic foams by employing the dissolution-sintering process but it was only applied as a slurry stabilizer during the production of ceramic foams [19]. The present paper aims to determine the influence of sintering process conditions on the microstructure of the resultant foam with a view to produce ceramic foams of high-quality and strength. One of the scopes of the present study is to evaluate the effect of vanadium oxide addition in the initial powder mixture with respect to the microstructural characteristics of the resulting ceramic foam. The above produced alumina–vanadia foams can have potential use as catalysts involved in partial or selective oxidation processes.

2. Experimental procedures

Alumina powder with a particle size of 110 μm and vanadium pentoxide with a particle size of 4 μm, both supplied by Alpha Aesar company, were used as the parent materials in this study. Commercial crystalline raw cane sugar with a mean particle size of 700 μm was used as a space holder material. The particle size of the sugar particles defines the pore size of the final foam. Several mixtures consisting of Al_2O_3 and V_2O_5 were prepared with molar ratios of 4, 16, and 32 mol% V_2O_5 aiming to investigate the effect of vanadium oxide addition on the microstructural characteristic of the produced foam.

The manufacturing process consists of four stages: mixing, compaction, dissolution and sintering. Initially, the ceramic powders are thoroughly mixed at a pre-specified weight ratio so as to obtain a 65% porosity, while an amount of binder (about 10% in weight) was added in the mixture. A solution of 20 wt% of cellulose acetate in acetone was used as a binder. Mixing yields in a homogeneous distribution of different ceramic powders and the space-holder material, ensuring the fabrication of high-quality foams with uniform pore size distributions.

The powder mixture was uniaxially pressed at a given pressure in a stainless steel cylindrical mold with a diameter of 16 mm and height of 80 mm. The sugar particles were removed from the green compact by water leaching. The final stage involves binder thermal removal and sintering performed in a high-temperature furnace. The thermal cycle was designed on the basis of the degradation temperature range of the binder, whilst preserving simultaneously the macro-pore network practically unchanged. Preforms were sintered at different temperatures (500, 800 and 1100 °C) during 1, 4 and 24 h in order to study the influence of the sintering conditions on the microstructure of the resultant foam.

The produced foam samples were sliced with a diamond saw and then polished with 3 and 6 μm diamond pastes. Optical microscopy (OM) and scanning electron microscopy (SEM) were used to characterize the cell wall microstructure of the produced foam. X-Ray diffraction (XRD) analysis was also performed to explain the final crystal structure of the ceramic foam. For the optical examinations, the foam specimens were embedded in a cold-hardening epoxy resin before polishing and were examined using a Leica DM 4000M microscope. The SEM study took place in a JEOL 840A scanning electron microscope working at 20 kV using the back scattered electron method and energy dispersive X-ray (EDX) analysis. For the XRD study a 2-cycle diffractometer (Philips PW 1050) with CuKa radiation was employed. Weight measurements were also carried out to determine the dissolution percentage of the sugar in the foam using an electronic balance with an accuracy of 0.001 g.

The porosity of the as-manufactured ceramic foam P_f can be evaluated by $P_f = 1 - \rho_f/\rho_s$, where ρ_f is the calculated density of the foam and ρ_s is the theoretical density of a fully dense Al_2O_3/V_2O_5 mixture. The density ρ_f of the final ceramic foam was calculated by dividing the mass of the foam by its volume, which was estimated, based on the Archimedes principle. The theoretical density of the dense mixture, ρ_s, was calculated by the rule of mixtures:

$$\rho_s = \rho_{Al_2O_3} V_{Al_2O_3} + \rho_{V_2O_5}(1 - V_{Al_2O_3})$$

where $\rho_{Al_2O_3}$ and $\rho_{V_2O_5}$ are the densities of Al_2O_3 and V_2O_5 respectively ($\rho_{Al_2O_3} = 3.967\ g/cm^3$ and $\rho_{V_2O_5} = 3.357\ g/cm^3$) and $V_{Al_2O_3}$ is the volume fraction of Al_2O_3 in the Al_2O_3/V_2O_5 powder mixture.

3. Results and discussion

3.1. Establishment of production conditions

The V_2O_5 powder has a high tendency to agglomerate due to its small particle size. The latter, however, is useful in improving sintering densification, since it can cover the larger in size alumina particles thus providing a strong bond between the ceramic powders during sintering. This can be ascribed to the melting phase created during the V_2O_5–Al_2O_3 reaction at

temperatures above 750 °C (for the examined molar ratios). The use of cellulose acetate binder at the mixing process was necessary in order to:

- avoid segregation of dissimilar powders during the mixing process,
- provide the required cohesion between different ceramic powders in order to retain the shape of the green product after the compaction stage and the subsequent dissolution process, and
- act as a lubricant during the compaction stage and facilitate uniform pressure distribution within the die.

However, the simultaneous mixing of the ceramic powders, sugar and binder should be avoided since it leads to the partial or total coverage of the sugar particles by the binder deterring their subsequent water dissolution. To facilitate the removal of the sugar particle during the dissolution stage, the mixing process was carried out in two stages: Firstly, V_2O_5 and Al_2O_3 powders were mixed with an amount of binder (~8% in weight) to create a homogeneous mixture. Secondly, the sugar particles were gradually added and mixed.

Uniaxial cold pressing was employed to form the green compacts using a stainless steel cylindrical die with a diameter of 16 mm and height of 80 mm. The optimum compaction pressure lies in the range of 300 MPa. Higher compaction pressures result in reduced powder bonding, since an extended amount of binder is squeezed out of the die.

Water leaching was conducted at 80 °C for 1 h achieving at least 95% removal of the sugar particles. The amount of crystalline raw sugar leached was determined by comparison of the mass of the preform and the initial mass of the ceramic powders. Although V_2O_5 is dissolvable in water, the reduced leaching process duration along with the limited dissolution rate of V_2O_5 in water (compared to that of sugar) ensured the minimal alteration of the initial ceramic powder ratio in the mixture. In this context, the protective shield formed by the binder, acts against water penetration in V_2O_5.

Binder removal was carried out by a thermal process. The thermal elimination of binder was optimized taking into account the degradation temperature range of the cellulose binder obtained by literature data [20]. It was found that the cellulose acetate has a gradual and quite wide decomposition temperature range (from 200 to 350 °C), which is beneficial from a technological point of view at least for two reasons: (i) in the initial stage the remaining binder component will serve to retain the shape of the foam and (ii) allows a smooth way out of decomposition products. Moreover, a wider temperature range decomposition stage allows for avoiding the formation of cracks during the process [9].

The optimized thermal cycle was established on the basis of try and error technique, and taking into account that high heating rates lead to the formation of cracks into the sample that might cause their partial or total collapse. Up to 400 °C, the heating rate was critical and had to be slow enough to prevent cracks, since the binder component decomposes. After several experiments it was found that a heating rate of 10 °C/min is appropriate for the specific temperature range, whilst a dwelling time of 40 min is adequate. Higher heating rates produced typical defects seen in Fig. 1a. These cracks are caused by pressure concentration and temperature gradients inside the preform compact, leading to partial or total collapse of the foam. Finally, the last heating up from 400 °C to the final temperature (800 or 1100 °C) takes place at a heating rate of 20 °C/min. Higher heating rates can lead to partial collapse of the foam due to rapid decomposition of any remaining binder or space holder material (sugar). The optimized two-step thermal cycle is shown in Fig. 1b. The dwelling time of the final heating stage (sintering stage) was varied from 1 to 24 h in order to investigate its effect on the foam's microstructure. The overall structure of ceramic foam produced under optimum thermal conditions is shown in Fig. 2. The pore size of the foam is similar to that of the sugar particle. It should be noted that the color of the preform foams changes from yellow to gray after the heat treatment in air, indicating a change in the chemical composition or creation of new phases.

Several mixtures consisting of the Al_2O_3 and V_2O_5 oxides were prepared with molar ratios of 4, 16, and 32 mol% V_2O_5 to investigate the microstructural characteristic of the produced foam. Foams with 4% V_2O_5 molar addition presented low strength since the amount of vanadium oxide was not adequate to provide sufficient bonding to the Al_2O_3 particles. Foams having V_2O_5 molar ratio higher than 32% were totally or partially melted when sintering temperature was above 750 °C. Sintering at lower temperatures (500 °C) yield to the production of yellow foams but requires excessively prolonged time

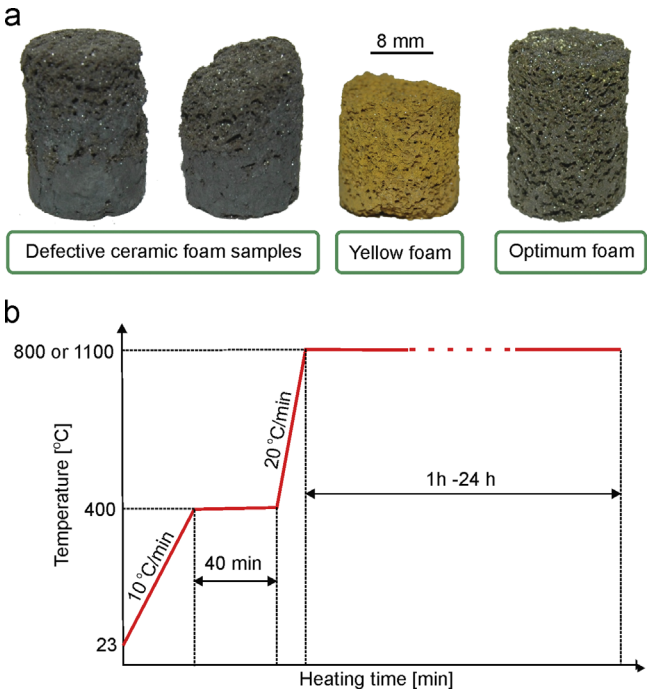

Fig. 1. (a) Typical ceramic foam samples having 65% porosity and 16 mol% V_2O_5 addition sintered under different heating conditions and (b) optimum thermal cycle for ceramic foam production.

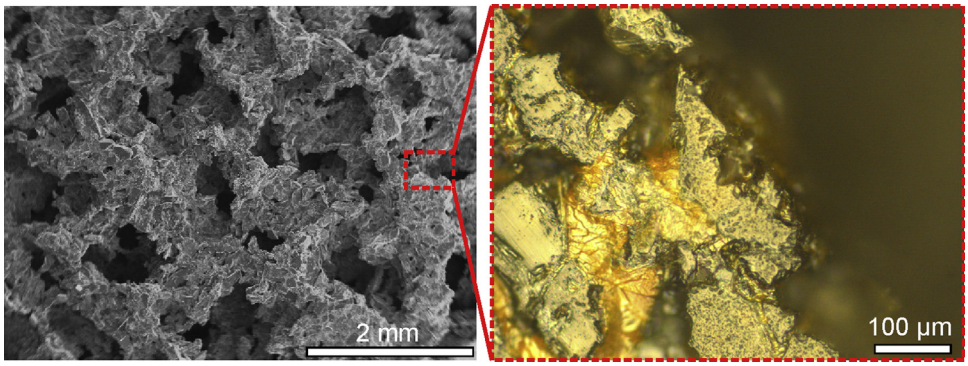

Fig. 2. Structure of Al_2O_3–16 mol% V_2O_5 foam having 65% porosity, produced under optimum thermal conditions. Sintering temperature of 1100 °C for 4 h.

(more than 48 h) in order to provide adequate strength so as to retain the foam structure intact.

Theoretically, the porosity of the ceramic foam is equivalent to the volume fraction of raw cane sugar in the initial ceramic powder/raw cane sugar preform, if the preform is 100% dense. The measured porosity of all samples is about 4–5% higher than the theoretical one. This difference can be partially attributed to the retained porosity created during the binder removal at the initial heating stage. However, another phenomenon is prevailing as well. It was observed that the dimensions of the final ceramic foam were slightly higher than those of the corresponding preforms indicating that not only shrinkage during sintering was negligible for all sintering conditions examined but also suggesting the existence of a mechanism provoking an increase in lattice parameters of Al_2O_3.

3.2. Microstructural analysis

3.2.1. XRD results

XRD techniques were undertaken in order to determine the microstructural analysis of the foams struts, within the possible reliability. The results presented in this investigation correspond to the specimens prepared with molar ratio of 16% V_2O_5, sintered at 1100 °C, due to the fact that this molar ratio results in best quality foams in a reasonable production time. Sintering time varied from 1 to 24 h while a rapid or slow cooling process was considered.

The phases developed during foam production, considering also the presence of polymorphs, were identified. X-ray diffraction patterns (Figs. 3–5) revealed overall a crystalline character for all the examined samples. After heat treatment the sample became black and shiny indicating a change in the chemical composition. Consequentially new weak reflections were observed in the X-ray pattern beside the lines stemming from Al_2O_3, and V_2O_5.

Peaks of Al_2O_3, V_2O_5 and $AlVO_4$ phases appeared in all samples irrespective of the amount of V_2O_5 in the initial mixture and processing conditions such as sintering time, temperature and cooling rate, which is consistent with the Al_2O_3–V_2O_5 phase diagram [21]. Equilibrium phases were also observed even after short reaction times (sintering time of 1 h) and rapid cooling (Fig. 3). More than 25 diffraction peaks were indexed to the rhombohedral corundum structure of

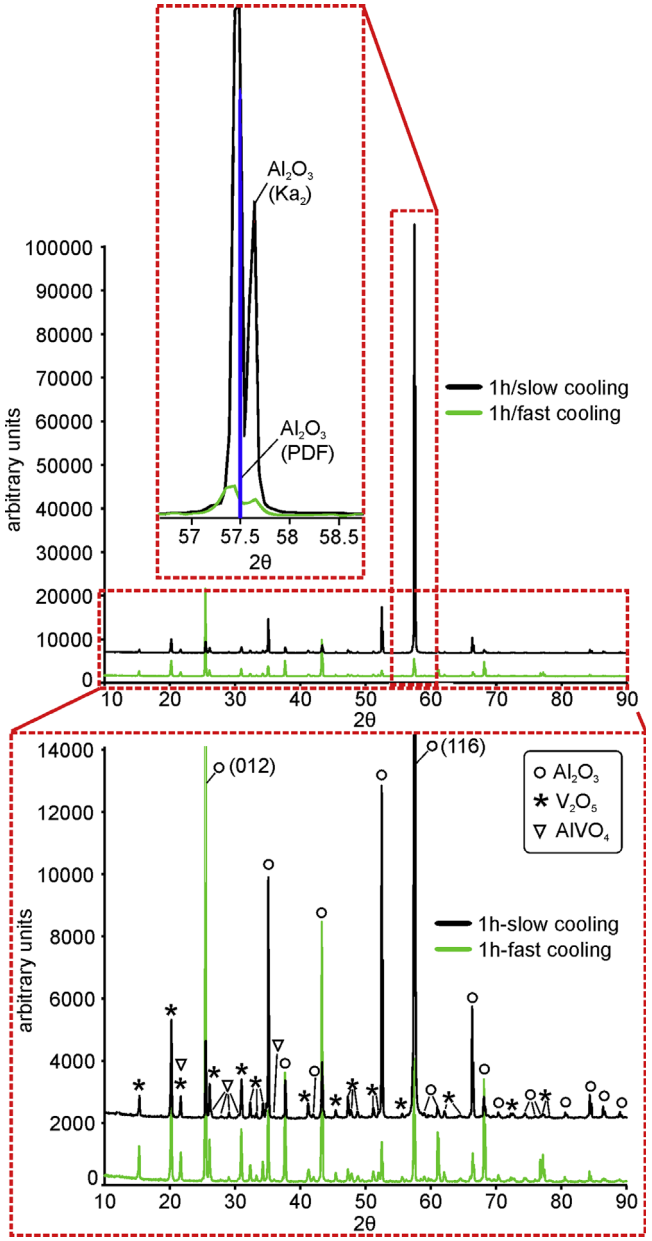

Fig. 3. X-ray diffraction pattern using CuKa radiation obtained for alumina foams having 16 mol% V_2O_5 and 65% porosity. Sintering temperature of 1100 °C for 1 h. (For interpretation of the references to color in this figure legend, the reader is referred to the web version of this article.)

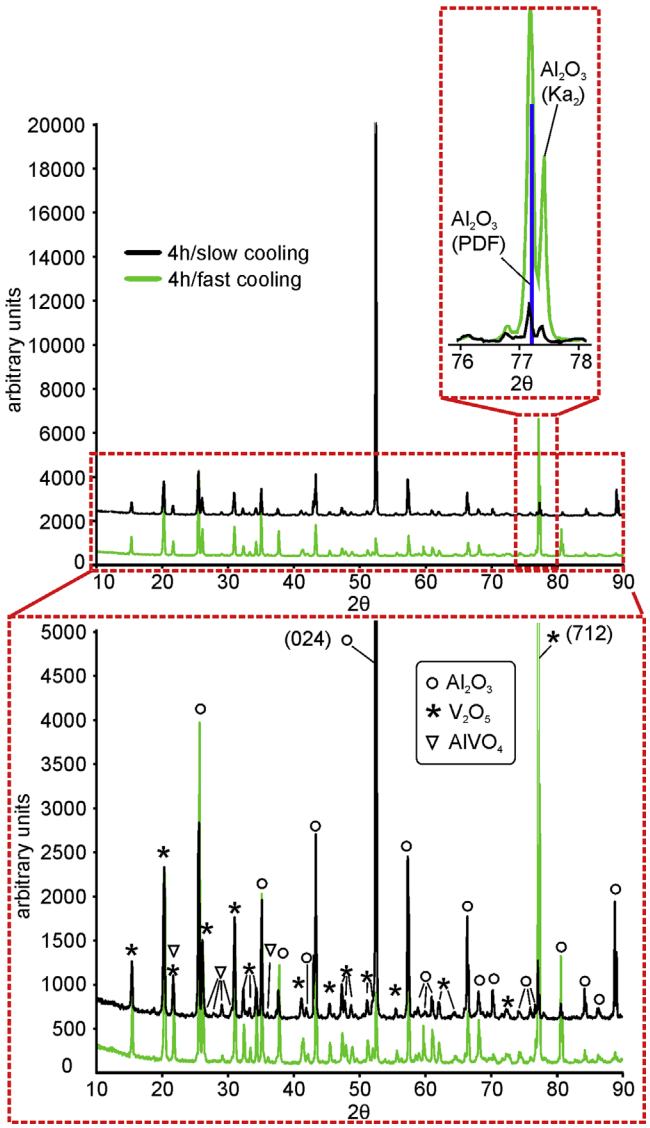

Fig. 4. X-ray diffraction pattern using CuKa radiation obtained for alumina-foams having 16 mol% V_2O_5 and 65% porosity. Sintering temperature of 1100 °C for 4 h. (For interpretation of the references to color in this figure legend, the reader is referred to the web version of this article.)

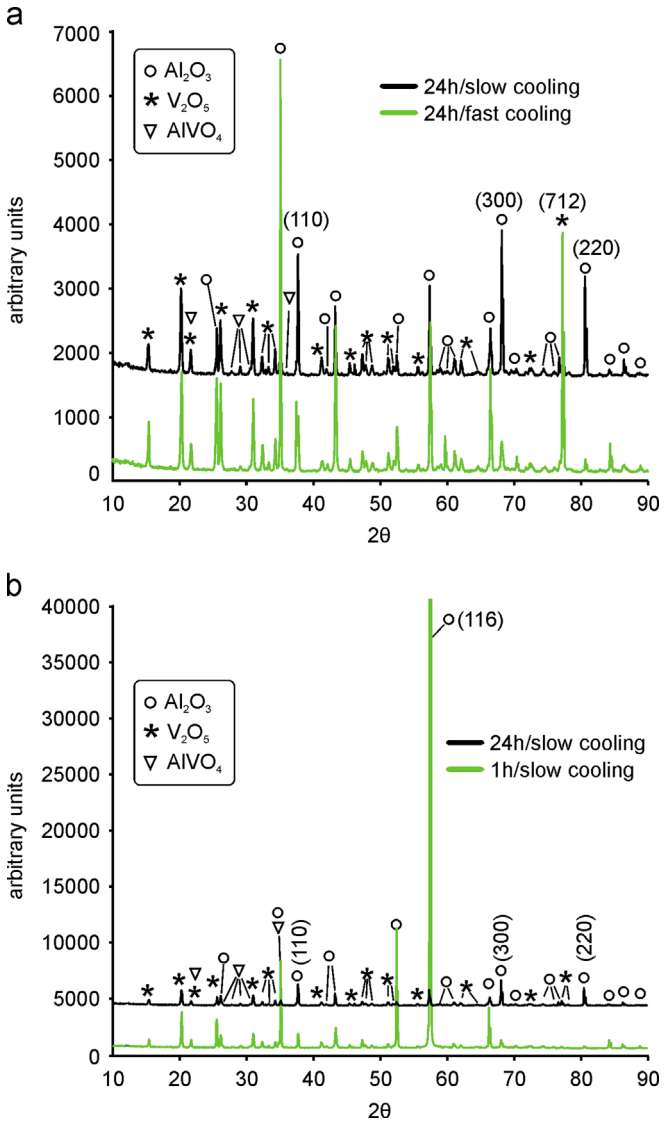

Fig. 5. X-ray diffraction pattern using CuKa radiation obtained for alumina-foams having 16 mol% V_2O_5 and 65% porosity. (a) Sintering temperature of 1100 °C for 24 h. (b) Sintering temperature of 1100 °C for 1 and 24 h applying slow cooling rate. (For interpretation of the references to color in this figure, the reader is referred to the web version of this article.)

Al_2O_3 (setting in space group $R\bar{3}c$), being the only polymorph that could be identified. Concerning vanadium oxide more than 30 peaks were assigned to the orthorhombic vanadium pentoxide structure (setting in space group Pmmn).

The observation of $AlVO_4$ as a single phase, indicates that a chemical reaction between Al_2O_3 and V_2O_5 took place. The presence of V_2O_5 indicates that there was still vanadium oxide that has not reacted with Al_2O_3 even when a small quantity of vanadium oxide was used in the initial powder mixture.

Concerning the cooling rate it can be noted that for short reaction times (sintering time of 1 h) the only difference appears in the preferred orientation of the Al_2O_3 toward (116) at slow cooling and toward (012) at rapid cooling. The phase of V_2O_5 presents a normal crystal growth without any texturing (Fig. 3). When sintering time was increased to 4 h and 20 h the preferred orientation was again observed only for the phase of Al_2O_3 toward (024) and both (300) and (220) respectively for slow cooling. However, when the cooling rate increased, the opposite case is apparent for 4 and 24 h sintering time. It can be seen that rapid cooling induces texturing for the phase of V_2O_5 toward (712) for both sintering time (4 h and 24 h) while the phase of Al_2O_3 presents a normal crystal growth (Figs. 4 and 5a).

The X-ray intensities of the Al_2O_3 phase were much stronger when sintering time was short while they exhibit a significant reduction with the raise of sintering duration. However no such phenomenon was observed for V_2O_5 phase suggesting that most Al_2O_3 particles were covered by the liquid phase of V_2O_5, being thus responsible for the attenuation of Al_2O_3 phase intensities (Fig. 5b).

The crystallite size D of Al_2O_3 was approximated using Sherrer's equation, $D = 0.9\lambda/(b \cos\theta)$, where λ is the

wavelength of X-ray, β is the Full Width at Half Maximum peak intensity (FWHM), and θ is Bragg's angle of diffraction. Several peaks in each sample were used while the average Sherrer's crystallite size is reported in Table 1.

Regarding the crystallite size of Al_2O_3 it can be concluded that longer sintering times and slow cooling rates favor the crystal growth of Al_2O_3 phase resulting in large grains as indicated by the sharp peaks of XRD patterns marked by black color in Figs. 3–5. On the other hand relatively broad peaks appeared at XRD patterns marked by green color in Figs. 3–5, accounting for short sintering time and fast cooling rate.

Table 1
Estimation of crystallite size of Al_2O_3.

Sintering time (h)	Slow cooling (nm)	Fast cooling (nm)
1	55	40
4	60	50
24	90	70

While most of the features could be accounted by the XRD fitting process, the peaks of Al_2O_3 phase exhibit diffused profiles indicating the presence of compositional fluctuations. Careful observations of the obtained XRD spectra reveals a small shift of the Al_2O_3 peaks toward smaller diffraction angles (insets of Figs. 3 and 4) with respect to the data obtained from the Powder Diffraction File Standards (PDFs), thus suggesting an increase in lattice parameters. It has been proposed that during the heating above 450 °C V_2O_5 is reduced and transforms to other vanadium oxides, but at the cooling stage it is oxidized again to V_2O_5 [13,22]. Taking into account that the incorporation of an octahedral transition metal oxide is associated with the removal of Al^{3+} from the structure, the volume

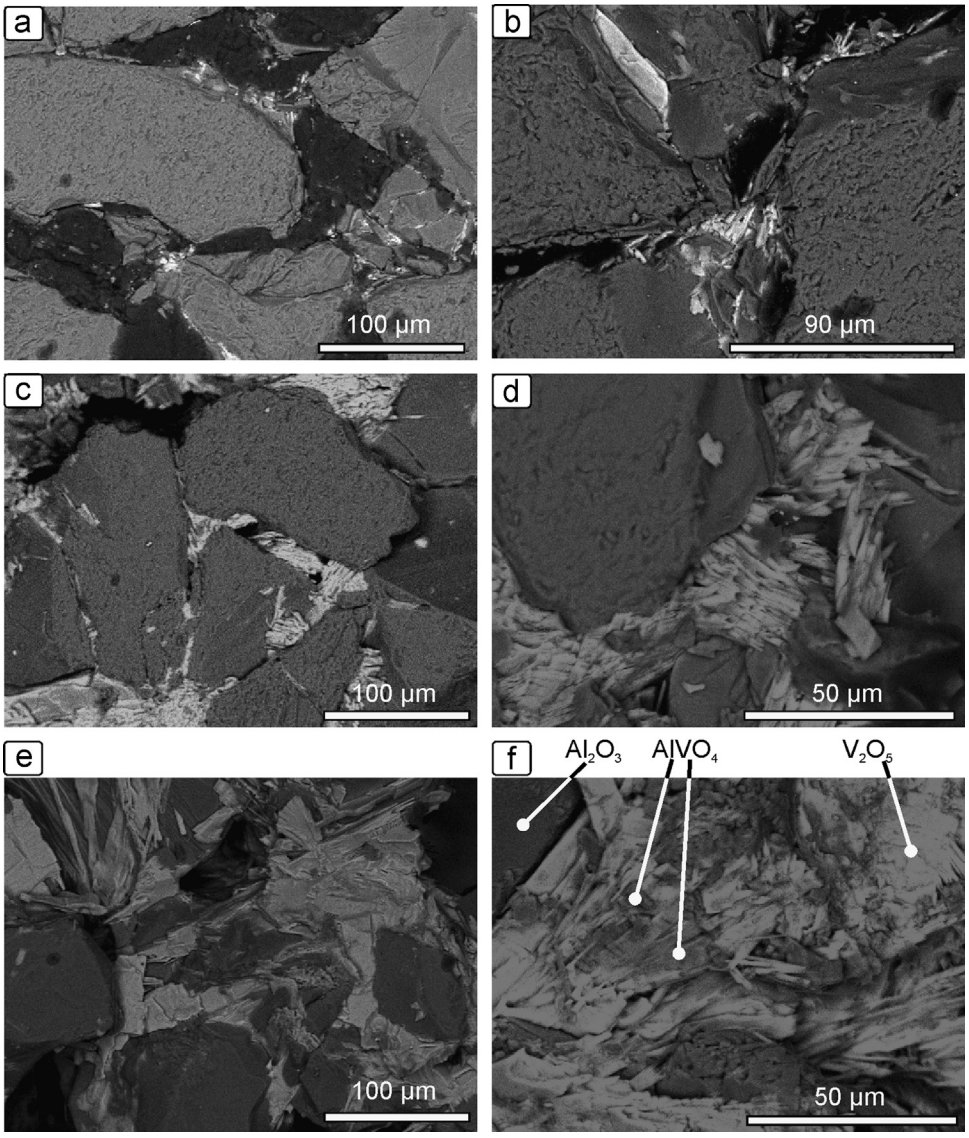

Fig. 6. SEM images of alumina foams cell walls with (a) 4 mol% V_2O_5 sintered at 800 °C for 4 h, (b) 4 mol% V_2O_5 sintered at 1100 °C for 4 h, (c) 16 mol% V_2O_5 sintered at 800 °C for 4 h, (d) 16 mol% V_2O_5 sintered at 1100 °C for 4 h, (e) 16 mol% V_2O_5 sintered at 1100 °C for 4 h showing a continuous network of the melted phase and (f) 16 mol% V_2O_5 sintered at 800 °C for 24 h.

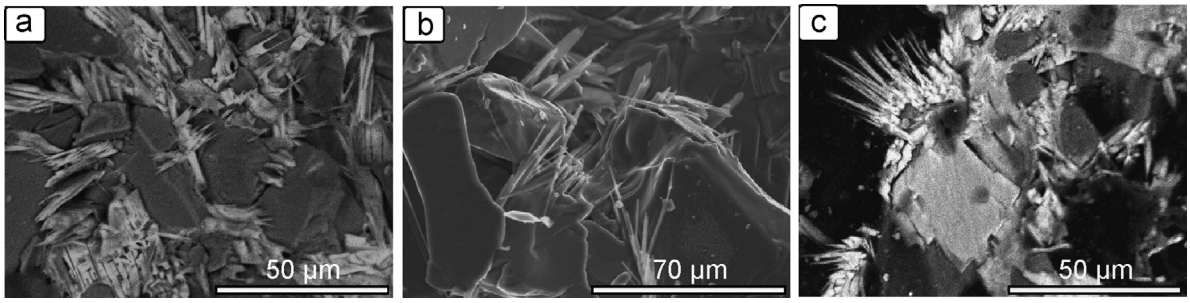

Fig. 7. SEM images of alumina foams cell walls with (a) 16 mol% V_2O_5 sintered at 800 °C for 4 h, (b) 16 mol% V_2O_5 sintered at 1100 °C for 4 h and (c) 4 mol% V_2O_5 sintered at 1100 °C for 4 h showing the whisker-shaped V_2O_5 crystal.

expansion of the ceramic foam can be explained if assuming that a small extent of Al^{3+} can be replaced by the larger V^{3+} or V^{4+}, which has an effective ionic radii of (0.74 Å) and (0.63 Å), larger than that of Al^{3+} (0.53 Å). Similar phenomena have been reported in literatures related with the reaction of V_2O_5 with other oxides such us TiO_2, $MgAl_2O_4$ spinel and yttria-stabilized zirconia [13,22–24].

3.2.2. SEM images

Fig. 6a–d shows a typical microstructure of the cell wall of the produced alumina foams having 4% and 16% molar addition of V_2O_5 sintered for 4 h at two different temperatures. The cell walls in the alumina foams with 4% molar addition of V_2O_5 present a considerable amount of voids and interstices, most of them originated from the compaction stage and are retained after sintering for both sintering temperatures (800 and 1100 °C). This indicates that the amount of V_2O_5 is not sufficient so as to fill the spaces between Al_2O_3 particles and generate a strong bonding among them. Consequently, a prolonged sintering period is required for establishing satisfactory bonding and adequate strength to the produced ceramic foam. The voids are considerably reduced when the amount of V_2O_5 is increased from 4 to 16 mol% By increasing the sintering temperature from 800 to 1100 °C, the cell walls became denser and only a limited number of micro-voids could be detected. Fig. 6e reveals the presence of continuous network of melted phase around each Al_2O_3 particle in such a case.

Microstructural investigation verified the presence of $AlVO_4$, consistent with XRD results. Upon contacting the vanadium oxide melt, the microstructure of the Al_2O_3 particles undergoes a surface change due to a dissolution–precipitation reaction, suggesting diffusion of Al ions that are dissolved by the liquid V_2O_5, and precipitate out as clusters. Based on EDX analysis, a compositional variation was detected in the melt area around Al_2O_3 particles as shown in Fig. 6f. A phase rich in Al, V, and O appears, corresponding to the high-contrast dark gray regions which can be assigned to $AlVO_4$ in accordance with the XRD results. It can be observed that the phase $AlVO_4$ is found not only near Al_2O_3 particles where the V_2O_5 melt is abundant, but also at a certain distance from the surface of Al_2O_3 particles, thus reflecting the diffusion depth of the Al ion which can form stable phases.

SEM observations of foam struts located at internal pores (and not at the polished cross-section of the foam) revealed the actual grain geometry of V_2O_5. V_2O_5 presents an elongated whisker-shaped crystal geometry irrespective of the sintering temperature, time and cooling rate (Fig. 7a and b). This is obvious even when the molar addition of V_2O_5 in the initial powder mixture is small (Fig. 7c). The length of the whisker-shaped V_2O_5 crystal is slightly increased with sintering temperature (Fig. 7a and b).

4. Conclusions

In this study, tailored made open-cell alumina–vanadia foams were produced by employing a dissolution sintering process, using crystalline raw cane sugar as a leachable pore former material. The influence of sintering process conditions (temperature, time and cooling rate) and V_2O_5 molar fraction were investigated. From this study the following conclusions can be drawn:

1. Crystalline raw cane sugar can be successfully used as a space-holder material for manufacturing ceramic foams by a dissolution-sintering process. Tuning of the volume fraction and size of raw cane sugar particles can tailor theoretical porosities, pore size and internal architecture of the foam.
2. V_2O_5 addition (around 16 mol%) in the alumina powder mixture results in enhanced sinterability and stability of the produced foam through reaction sintering and creation of liquid phases.
3. The crystal size of Al_2O_3 showed a dependency on the cooling rate and sintering time of the production process.
4. Different texturing-preferred orientations were observed for the crystal growth of V_2O_5 and Al_2O_3 phases depending on the cooling rate and sintering time.
5. A volume expansion of the ceramic foam was observed, verified also by XRD measurements, attributed mainly to the substitution of Al^{3+} by larger vanadium cations.

References

[1] M. Scheffler, P. Colombo, Cellular Ceramics: Structure, Manufacturing, Properties and Applications, WILEY-VCH Verlag GmbH & Co. KGaA, Weinheim, 2005.

[2] N. Michailidis, F. Stergioudi, H. Omar, E. Paulidou, D.N. Tsipas, C. Albanakis, D. Missirlis, B. Granier, Microstructural characterization of oxide morphologies on Ni and Inconel foams exposed to concentrated solar radiation, Journal of Alloys and Compounds 496 (2010) 644–649.

[3] I. Garrn, C. Reetz, N. Brandes, L.W. Kroh, H. Schubert, Clot-forming: the use of proteins as binders for producing ceramic foams, Journal of the European Ceramic Society 24 (2004) 579–587.
[4] J. Wang, Y. Huang, J. Lu, H. Chen, Effect of binder on the structure and mechanical properties of lightweight bubble alumina ceramic, Ceramics International 38 (2012) 657–662.
[5] R. Faure, F. Rossignol, T. Chartier, C. Bonhomme, A. Maître, G. Etchegoyen, P. Del Gallo, D. Gary, Alumina foam catalyst supports for industrial steam reforming processes, Journal of the European Ceramic Society 31 (2011) 303–312.
[6] T. Isobe, T. Tomita, Y. Kameshima, A. Nakajima, K. Okada, Preparation and properties of porous alumina ceramics with oriented cylindrical pores produced by an extrusion method, Journal of the European Ceramic Society 26 (2006) 957–960.
[7] F. Tang, H. Fudouzi, T. Uchikoshi, Y. Sakka, Preparation of porous materials with controlled pore size and porosity, Journal of the European Ceramic Society 24 (2004) 341–344.
[8] G.Incera Garrido, F.C. Patcas, S. Lang, B. Kraushaar-Czarnetzki, Mass transfer and pressure drop in ceramic foams: a description for different pore sizes and porosities, Chemical Engineering Science 63 (2008) 5202–5217.
[9] P. Thomas-Vielma, A. Cervera, B. Levenfeld, A. Varez, Production of alumina parts by powder injection molding with a binder system based on high density polyethylene, Journal of the European Ceramic Society 28 (2008) 763–771.
[10] K. Ghillányová, D. Galusek, M. Pentrák, J. Madejová, I. Bertóti, J. Szépvölgyi, P. Šajgalík, The influence of ageing on consolidation and sinterability of a sub-micron alumina powder, Powder Technology 214 (2011) 313–321.
[11] M.H. Bocanegra-Bernal, C. Domınguez-Rios, A. Garcia-Reyes, A. Aguilar-Elguezabal, J. Echeberria, A. Nevarez-Rascon, Fracture toughness of an a-Al_2O_3 ceramic for joint prostheses under sinter and sinter-HIP conditions, International Journal of Refractory Metals and Hard Materials 27 (2009) 722–772.
[12] J.-H. Li, H.-W. Ma, W.-H. Huang, Effect of V_2O_5 on the properties of mullite ceramics synthesized from high-aluminum fly ash and bauxite, Journal of Hazardous Materials 166 (2009) 1535–1539.
[13] M.R. Bayati, R. Molaei, A.Z. Moshfegh, F. Golestani-Fard, A strategy for single-step elaboration of V_2O_5-grafted TiO_2 nanostructured photocatalysts with evenly distributed pores, Journal of Alloys and Compounds 509 (2011) 6236–6241.
[14] Y.H. Taufiq-Yap, K.C. Waugh, A study of the nature of the oxidant in V_2O_5–MoO_3/Al_2O_3 catalyst, Chemical Engineering Science 56 (2001) 5787–5792.
[15] L.B. Kong, Y.B. Gan, J. Ma, T.S. Zhang, F. Boey, R.F. Zhang, Mullite phase formation and reaction sequences with the presence of pentoxides, Journal of Alloys and Compounds 351 (2003) 264–272.
[16] B. Schimmoeller, H. Schulz, S.E. Pratsinis, A. Bareiss, A. Reitzmann, B. Kraushaar-Czarnetzki, Ceramic foams directly-coated with flame-made V_2O_5/TiO_2 for synthesis of phthalic anhydride, Journal of Catalysis 243 (2006) 82–92.
[17] N. Michailidis, F. Stergioudi, D.N. Tsipas, Manufacturing of open-cell metal foams using a novel leachable pattern, Advanced Engineering Materials 13 (2011) 29–32.
[18] N. Michailidis, F. Stergioudi, Establishment of process parameters for producing Al-foam by dissolution and powder sintering method, Materials and Design 32 (2011) 1559–1564.
[19] M. Pradhan, P. Bhargava, Effect of sucrose on fabrication of ceramic foams from aqueous slurries, Journal of the American Ceramic Society 88 (2005) 216–218.
[20] M.C.C. Lucena, A.E.V. de Alencar, S.E. Mazzeto, S.A. Soares, The effect of additives on the thermal degradation of cellulose acetate, Polymer Degradation and Stability 80 (2003) 149–155.
[21] G. Dabrowska, P. Tabero, M. Kurzawa, Phase relations in the Al_2O_3–V_2O_5–MoO_3 system in the solid state. The crystal structure of $AlVO_4$, Journal of Phase Equilibria and Diffusion 30 (2009) 220–229.
[22] B. Fernandez, J.M. Almanza, J.L. Rodrıguez, D.A. Cortes, J.C. Escobedo, E.J. Gutierrez, Corrosion mechanisms of $Al_2O_3/MgAl_2O_4$ by V_2O_5, NiO, Fe_2O_3 and vanadium slag, Ceramics International 37 (2011) 2973–2979.
[23] S. Hoffmann, S.T. Norberg, M. Yoshimura, Melt synthesis of Al_2TiO_5 containing composites and reinvestigation of the phase diagram Al_2O_3–TiO_2 by powder X-ray diffraction, Journal of Electroceramics 16 (2006) 327–330.
[24] Z. Chen, S. Speakman, J. Howe, H. Wang, W. Porter, R. Trice, Investigation of reactions between vanadium oxide and plasma-sprayed yttria-stabilized zirconia coatings, Journal of the European Ceramic Society 29 (2009) 1403–1411.